

UC Berkeley

UC Berkeley Previously Published Works

Title

In planta production of the nylon precursor beta-ketoadipate

Permalink

<https://escholarship.org/uc/item/6g61625x>

Authors

Kazaz, Sami

Tripathi, Jaya

Tian, Yang

et al.

Publication Date

2025-04-01

DOI

10.1016/j.jbiotec.2025.04.008

Copyright Information

This work is made available under the terms of a Creative Commons Attribution License, available at <https://creativecommons.org/licenses/by/4.0/>

Peer reviewed



Contents lists available at ScienceDirect

Journal of Biotechnology

journal homepage: www.elsevier.com/locate/jbiotec

In planta production of the nylon precursor beta-ketoadipate

Sami Kazaz^{a,b}, Jaya Tripathi^{a,c}, Yang Tian^{a,b}, Halbay Turumtay^{a,b}, Dylan Chin^{a,b,d}, İrem Pamukçu^{a,b,e}, Monikaben Nimavat^{a,c}, Emine Akyuz Turumtay^{a,c}, Edward E.K. Baidoo^{a,c}, Corinne D. Scown^{a,c,f,g}, Aymerick Eudes^{a,b,*}

^a Joint BioEnergy Institute, EmeryStation East, 5885 Hollis St, 4th Floor, Emeryville, CA 94608, USA

^b Environmental Genomics and Systems Biology Division, Lawrence Berkeley National Laboratory, 1 Cyclotron Road, Berkeley, CA 94720, USA

^c Biological Systems and Engineering Division, Lawrence Berkeley National Laboratory, 1 Cyclotron Road, Berkeley, CA 94720, USA

^d Rausser College of Natural Resources, University of California-Berkeley, Berkeley, CA 94720, USA

^e Department of Molecular and Cell Biology, University of California-Berkeley, Berkeley, CA 94720, USA

^f Energy & Biosciences Institute, University of California-Berkeley, Berkeley, CA 94720, USA

^g Energy Analysis and Environmental Impacts Division, Lawrence Berkeley National Laboratory, Berkeley, CA 94720, USA

ARTICLE INFO

Keywords:

Beta-ketoadipate
Bioproduct
Plant engineering
Shikimate pathway
Lignin
Techno-economic analysis

ABSTRACT

Beta-ketoadipate (βKA) is an intermediate of the βKA pathway involved in the degradation of aromatic compounds in several bacteria and fungi. Beta-ketoadipate also represents a promising chemical for the manufacturing of performance-advantaged nylons. We established a strategy for the *in planta* synthesis of βKA via manipulation of the shikimate pathway and the expression of bacterial enzymes from the βKA pathway. Using *Nicotiana benthamiana* as a transient expression system, we demonstrated the efficient conversion of protocatechuate (PCA) to βKA when plastid-targeted bacterial-derived PCA 3,4-dioxygenase (PcaHG) and 3-carboxy-*cis,cis*-muconate cycloisomerase (PcaB) were co-expressed with 3-deoxy-D-arabinoheptulosonate 7-phosphate synthase (AroG) and 3-dehydroshikimate dehydratase (QsuB). This metabolic pathway was reconstituted in *Arabidopsis* by introducing a construct (*pAtβKA*) with stacked *pcaG*, *pcaH*, and *pcaB* genes into a PCA-overproducing genetic background that expresses AroG and QsuB (referred as *QsuB-2*). The resulting *QsuB-2* × *pAtβKA* stable lines displayed βKA titers as high as 0.25 % on a dry weight basis in stems, along with a drastic reduction in lignin content and improvement of biomass saccharification efficiency compared to wild-type controls, and without any significant reduction in biomass yields. Using biomass sorghum as a potential crop for large-scale βKA production, techno-economic analysis indicated that βKA accumulated at titers of 0.25 % and 4 % on a dry weight basis could be competitively priced in the range of \$2.04–34.49/kg and \$0.47–2.12/kg, respectively, depending on the selling price of the residual biomass recovered after βKA extraction. This study lays the foundation for a more environmentally-friendly synthesis of βKA using plants as production hosts.

1. Introduction

Nylon-6,6 is a synthetic polyamide resulting from the thermally-induced polycondensation between hexamethylenediamine (HMDA) and adipic acid (Vagholkar, 2016). Its unique physical and thermochemical properties revolutionized the polymer and plastic industries at the time of its invention (Varghese and Grinstaff, 2022). Currently, adipic acid production mainly relies on the nitric acid-catalyzed oxidation of petroleum-derived ketone-alcohol (KA) oil, a process that emits

nitrous oxide, which is a potent greenhouse gas (GHG) (Hasanbeigi and Sibal, 2023; Shimizu et al., 2000). Around three million tons of adipic acid are produced annually, emitting approximately 4.5 kg CO₂-equivalent (CO₂e) per kg adipic acid on a life-cycle basis, and the demand is anticipated to grow over the next decades, driven by the automotive industry and the furniture and bedding markets (Nicholson et al., 2023; Kondo et al., 2022). Developing more renewable, lower-emitting approaches to produce adipic acid or using other dicarboxylic acids to make nylon-6,6 analogs have consequently emerged as major focal point

Abbreviations: βKA, beta-ketoadipate; LC-MS, liquid chromatography-mass spectrometry; MSP, minimum selling price; PCA, protocatechuate; SMB, simulated moving bed; TEA, techno-economic analysis.

* Corresponding author at: Joint BioEnergy Institute, EmeryStation East, 5885 Hollis St, 4th Floor, Emeryville, CA 94608, USA.

E-mail address: ageudes@lbl.gov (A. Eudes).

<https://doi.org/10.1016/j.jbiotec.2025.04.008>

Received 4 February 2025; Received in revised form 6 April 2025; Accepted 9 April 2025

Available online 12 April 2025

0168-1656/© 2025 The Author(s). Published by Elsevier B.V. This is an open access article under the CC BY license (<http://creativecommons.org/licenses/by/4.0/>).

for the bioeconomy (Polen et al., 2013; Yan et al., 2023).

Beta-ketoadipate (β KA), a C6 dicarboxylic acid with a β -ketone group, is an intermediate of the β KA catabolic pathway responsible for the conversion of aromatic compounds into tricarboxylic acid cycle intermediates in several soil bacteria and fungi (Harwood and Parales, 1996; Wells and Ragauskas, 2012). Due to its structural similarity with adipic acid, β KA represents a promising building block chemical that can be efficiently reacted with HMDA to produce nylon-6,6 analogs (referred as nylon-6, β K6) (Johnson et al., 2019; Rorrer et al., 2022). This nylon-6, β K6 polyamide displayed favorable properties compared to its adipic acid counterpart. For example, nylon-6, β K6 has lower water permeability relative to nylon-6,6, making it comparable to sebacic acid-derived nylon-6,10, yet it also features a higher glass transition temperature than nylon-6,10 (Rorrer et al., 2022).

Several bioengineering strategies have already been implemented for the production of β KA from various precursor molecules by leveraging the β KA pathway, using mostly *Pseudomonas putida* KT2440 as a microbial host. Generally, these strategies consist of the inactivation of the β KA:succinyl-coenzyme A transferase (PcaIJ) within the pathway to prevent β KA conversion and enable its accumulation. Depending on their structure and the upper catabolic pathways involved, aromatic precursors can feed the β KA pathway either via the protocatechuate (PCA) or the catechol branches. As a notable example, β KA could be produced in *P. putida* KT2440 from polystyrene-derived benzoate via the catechol branch (Sullivan et al., 2022). Other examples leveraged the PCA branch to produce β KA from PCA (Okamura-Abe et al., 2016), 4-hydroxybenzoate (Johnson et al., 2019), *p*-coumarate (Fenster et al., 2022), ferulate (Werner et al., 2023), terephthalate (Sullivan et al., 2022; Werner et al., 2021), vanillin and vanillate (Suzuki et al., 2021), or even glucose (Rorrer et al., 2022).

Plants represent a compelling alternative to microbial hosts for the cost-effective production of chemicals given their ability to fix carbon from the atmosphere through photosynthesis and the possibility to grow them on a large scale (O'Neill and Kelly, 2017; Yang et al., 2022; Yuan and Grotewold, 2015). In plants, the shikimate pathway is source of precursors to secondary metabolites, including flavonoids, anthocyanins, salicylates, and polymers such as tannins and lignin (Maeda and Dudareva, 2012; Shende et al., 2024). Various engineering approaches enabling the production of valuable shikimate-derived compounds have been demonstrated, with a particular interest in simultaneously interfering with the lignin biosynthetic pathway (Liu and Eudes, 2022). Notable examples include the *in planta* production of the platform chemicals muconic acid (Eudes et al., 2018) and 2-pyrone-4,6-dicarboxylic acid (Lin et al., 2021), as well as the flavoring agent 2-phenylethanol (Qi et al., 2015). To the best of our knowledge, there is no report on the use of plants as platform hosts for β KA production. Therefore, we evaluated the potential of an *in planta* biological route for β KA synthesis from PCA using metabolic engineering and assisted by techno-economic analysis (TEA).

The engineered overproduction of PCA has been achieved in various plant species using plastid-targeted bacterial-derived enzymes to reroute the shikimate pathway. In particular, the expression of a 3-dehydroshikimate dehydratase (QsuB) from *Corynebacterium glutamicum* converted endogenous 3-dehydroshikimate into PCA in Arabidopsis stems (Eudes et al., 2015), leading to an increase in PCA content by up to 113-fold in comparison to the wild-type controls. This strategy was later implemented in tobacco (*Nicotiana tabacum* L.) (Wu et al., 2017) and bioenergy crops such as switchgrass (*Panicum virgatum* L.) (Hao et al., 2021), hybrid poplar (*Populus alba* x *grandidentata*) (Unda et al., 2022), and sorghum (*Sorghum bicolor* (L.) Moench) (Tian et al., 2022). The subsequent development of a transgenic Arabidopsis line (referred as *QsuB-2*) expressing a feedback-resistant 3-deoxy-D-arabinoheptulosonate 7-phosphate synthase (AroG) from *Escherichia coli* in addition to QsuB increased the carbon flux through the shikimate pathway and further enhanced PCA accumulation by ~8-fold in comparison to the transgenic plants only expressing QsuB (Umana et al., 2022). In the

current work, the approach for PCA overproduction was exploited and combined with the aforementioned β KA pathway previously employed in microbial studies to achieve β KA synthesis *in planta*.

To first validate β KA production *in planta*, we overproduced PCA in *Nicotiana benthamiana* leaves via transient expression of AroG and QsuB and partially reconstituted the PCA branch of the β KA pathway by co-expressing plastid-targeted versions of PcaHG, PcaB, PcaC, and PcaD derived from *P. putida* KT2440 (Fig. 1, route 1). An alternative engineered pathway for the conversion of PCA into β KA via the intermediate hydroxyquinol was also tested based on catabolic pathways previously reported in certain bacteria, yeast strains, and white-rot fungi (del Cerro et al., 2021; Holesova et al., 2011; Kitagawa et al., 2004; Spence et al., 2020). This latter consists of a promiscuous 4-hydroxybenzoate hydroxylase from *Candida parapsilosis* (MNX1), and hydroxyquinol 1, 2-dioxygenase (TsdC) and maleylacetate reductase (TsdD) from the γ -resorcyolate catabolic pathway in *Rhodococcus jostii* RHA1 (Holesova et al., 2011; Kasai et al., 2015) (Fig. 1, route 2). Successful production of β KA was achieved in the transformed *N. benthamiana* leaves, with the highest titers obtained via the PCA 3,4-cleavage route, and without the need of PcaC and PcaD expression (route 1). Further, this strategy implemented in Arabidopsis by transforming the PCA-overproducing line *QsuB-2* with stacked *pcaG*, *pcaH*, and *pcaB* genes led to a β KA production of up to ~0.25 dwt% in stems. Besides this value-added coproduct trait, biomass from engineered Arabidopsis lines has less lignin and displays improved saccharification efficiencies compared to the wild-type controls, which has the potential to lower the minimum selling price (MSP) of β KA produced thereof.

2. Material and methods

2.1. Chemicals

The antibiotics kanamycin, carbenicillin, chloramphenicol, and gentamicin were purchased from Teknova. Protocatechuate was purchased from Alfa Aesar. Beta-ketoadipate was purchased from Toronto Research Chemicals. All other chemicals were purchased from Sigma-Aldrich.

2.2. Plant material and growth conditions

The Arabidopsis transgenic line *QsuB-2* was previously described in Umana et al. (2022). Arabidopsis seeds were surface sterilized and sown on Murashige and Skoog medium (PhytoTechnology Laboratories) solidified with 0.8 % (w/v) agar. After a cold treatment of 48 h at 4 °C in the dark, plates were kept in a growth chamber (Percival Scientific; 16-h light/24 °C, 8-h dark/20 °C, 120 $\mu\text{mol m}^{-2} \text{s}^{-1}$). After 10 d, the seedlings were transferred to soil (Sun Gro Horticulture) in individual pots, grown in a growth chamber (Percival Scientific; 16-h light/24 °C, 8-h dark/20 °C, 150 $\mu\text{mol m}^{-2} \text{s}^{-1}$, 60 % relative humidity), and watered on a regular basis. The height of the main stem was measured at the mature senesced stage. The stems were harvested without leaves and siliques for total stem biomass dry weight measurements. Wild-type *Nicotiana benthamiana* seeds were directly germinated on soil and grown in a growth chamber as previously described (Lin et al., 2021).

2.3. Plasmid construction and plant transformation

The DNA coding sequences of PcaG, PcaH, PcaB, PcaC, and PcaD were codon-optimized for expression in Arabidopsis and synthesized (GenScript Biotech). All coding sequences contained at their 5'-end the sequence of a plastid transit peptide (schI) and flanking *BsaI* restriction sites for subcloning. The level-0 constructs are listed in Supplementary Table S1. For transient expression in *N. benthamiana*, synthetic sequences encoding schI-PcaG, schI-PcaH, schI-PcaB, schI-PcaC, and schI-PcaD were released by *BsaI* digest from the level-0 backbone and individually ligated into the binary vector pPMS057 containing a 35S

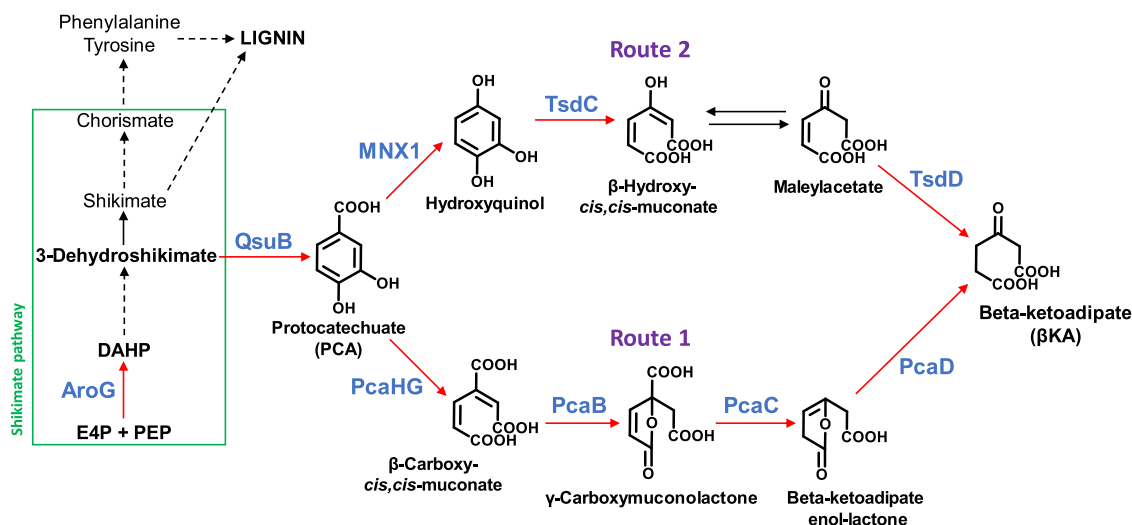


Fig. 1. A schematic diagram of the engineered metabolic pathways converting PCA to β KA in plant plastids. Red arrows represent biosynthetic steps catalyzed by microbial enzymes expressed in *N. benthamiana* and *Arabidopsis*. Dashed arrows denote multiple enzyme steps. AroG: feedback-resistant 3-deoxy-D-arabinoheptulosonate 7-phosphate (DAHP) synthase AroG^{L175Q}; E4P: erythrose 4-phosphate; MNX1: 4-hydroxybenzoate 1-hydroxylase; PcaB: 3-carboxy-*cis,cis*-muconate cyclisomerase; PcaC: 4-carboxymuconolactone decarboxylase; PcaD: 3-oxoadipate enol-lactonase; PcaHG: protocatechuate 3,4-dioxygenase; PEP: phosphoenolpyruvate; QsuB: 3-dehydroshikimate dehydratase; TsdC: hydroxyquinol 1,2-dioxygenase; TsdD: maleylacetate reductase.

promoter (*p35S*) from the cauliflower mosaic virus (Belcher et al., 2020). Codon-optimized synthetic sequences encoding *schl-MNX1*, *schl-TsdC*, and *schl-TsdD* were synthesized and cloned downstream *p35S* in pPMS057 directly (GenScript Biotech). The pPMS057 constructs containing *p35S::schl-AroG*, *p35S::schl-QsuB*, *p35S::schl-MNX1*, *p35S::schl-TsdC*, *p35S::schl-TsdD*, *p35S::schl-PcaG*, *p35S::schl-PcaH*, *p35S::schl-PcaB*, *p35S::schl-PcaC*, and *p35S::schl-PcaD* were individually electroporated into *Agrobacterium tumefaciens* GV3101 (pMP90) strain. Selection was made on Luria-Bertani solid medium supplemented with 50 $\mu\text{g ml}^{-1}$ kanamycin, 30 $\mu\text{g ml}^{-1}$ gentamicin, and 100 $\mu\text{g ml}^{-1}$ rifampicin. Leaves of 4-week-old *N. benthamiana* plants were infiltrated with *Agrobacterium* strains ($\text{OD}_{600} = 1.0$) carrying pPMS057 vectors of interest as previously described (Sparkes et al., 2006). All plasmids used for transient expression assays are listed in Supplementary Table S2.

For stable *Arabidopsis* transformation (ecotype Columbia 0), the jStack cloning approach was used to generate the level-2 construct *pAt β KA* (Shih et al., 2016). Coding sequences were amplified by PCR using the primers listed in Supplementary Table S3 and level-0 constructs as templates. The PCR products were digested with *BsaI* prior to ligation into the level-1 backbone PMS008 (Shih et al., 2016). Detailed information about the level-0 and level-1 plasmids used for jStack assembly are listed in Supplementary Table S1 and S4. The construct *pAt β KA* was introduced into the *Arabidopsis* line *QsuB-2* via *Agrobacterium*-mediated transformation (Bechtold and Pelletier, 1998). *QsuB-2* x *pAt β KA* primary T0 transformants were selected on MS medium containing 50 $\mu\text{g ml}^{-1}$ kanamycin. All plasmid sequences are available at the Inventory of Composable Elements (ICE) source registry (<http://public-registry.jbei.org>).

2.4. RNA extraction, cDNA preparation, and PCR analysis

The main stem from 4-week old plants (three plants per line) were flash-frozen in liquid nitrogen and ground into powder for total RNA extraction using the RNeasy Plant Mini Extraction Kit (Qiagen). RNA solutions were treated with 30 units of Dnase I Rnase-free (Qiagen) to remove residual genomic DNA and eluted with 30 μl of nuclease-free water. For reverse transcription (RT)-PCR, DNA-free RNA was converted to first-strand cDNA with the RevertAid H Minus First Strand cDNA Synthesis Kit (Fermentas) using oligo(dT)₂₂. Detection by PCR of the *aroG*, *qsuB*, *pcaG*, *pcaH*, *pcaB*, and *Actin 2* transcripts in the different *Arabidopsis* lines was conducted using the primers listed in

Supplementary Table S3.

2.5. Metabolite extraction

Metabolites were extracted from lyophilized *N. benthamiana* leaves and mature senesced and dried *Arabidopsis* stems using 80 % (v/v) methanol-water solvent as previously described (Eudes et al., 2018). For each sample, 30 mg of ball-milled biomass was sequentially extracted three times with 1 ml of solvent at 70 °C with shaking (2000 rpm) for 15 min. The 3-ml extracts were mixed with 1.5 ml of HPLC grade water and cleared by centrifugation at 3220 \times g for 5 min. Extracts were filtered through Amicon Ultra centrifugal filters (3 kDa MW cut off, EMD Millipore) at 13,000 \times g for 1.5 h. For PCA and hydroxyquinol quantification, a 250 μl aliquot of the filtered extracts was dried under vacuum and hydrolyzed with 1 N HCl for 2.5 h at 95 °C to release the aglycone forms, followed by three sequential ethyl acetate partitioning steps as previously described (Eudes et al., 2015).

2.6. Metabolite analysis

Metabolites were analyzed in plant extracts using liquid chromatography (LC), electrospray ionization (ESI), and quadrupole time-of-flight (QTOF) mass spectrometry (MS). LC-MS was performed via an Agilent Technologies 1260 Infinity HPLC system coupled to an Agilent Technologies 6520 Accurate-Mass QTOF LC/MS system. The HPLC sample tray, column compartment, and injection volume were set to 6 °C, 50 °C, and 3 μl , respectively. HPLC solvents A and B were 0.1 % formic acid in water and 0.1 % formic acid in methanol, respectively. Gradient elution was conducted as follows: linearly increased from 5 % solvent B to 60.9 % B in 4.3 min, increased from 60.9 % B to 97.1 % B in 1.3 min, held at 97.1 % B for 1 min, linearly decreased from 97.1 % B to 5 % B in 0.2 min, and held at 5 % B for 2 min. The flow rate was held at 0.42 ml min^{-1} for 5.6 min, increased from 0.42 ml min^{-1} to 0.65 ml min^{-1} in 0.2 min, and held at 0.65 ml min^{-1} for 2 min. The total LC run time was 8.8 min. For ESI, drying and nebulizer gases were set to 11 L min^{-1} and 20 lb/in^2 , respectively, and a drying gas temperature of 330 °C was used throughout. Electrospray ionization was conducted in the negative ion mode and a capillary voltage of 3500 V was utilized. The fragmentor, skimmer, and OCT 1 RF Vpp voltages were set to 100 V, 50 V, and 250 V, respectively. We found that β KA decarboxylates into levulinic acid under our LC-MS conditions. Quantification was made via

8-point calibration curves of authentic standards. The monoisotopic m/z (negative ionization) of hydroxyquinol, deprotonated PCA, β -hydroxycis,cis-muconate, maleylacetate, and levulinic acid (decarboxylated β KA) are 125.02315, 153.01933, 156.00697, 157.01425, and 115.04007, respectively.

2.7. Lignin measurements

Lignin was quantified from mature senesced and dried Arabidopsis stems using the thioglycolic acid method as previously described (Suzuki et al., 2009). Dried cell wall residues (~10 mg) obtained after sequential metabolite extractions were used (see 2.5).

2.8. Biomass pretreatment and saccharification

Ball-milled senesced Arabidopsis stems (~10 mg) were mixed in 340 μ l of water and shaken at 1400 rpm for 30 min at 30°C, followed by a 1 h incubation at 120°C for hot water pretreatment. Saccharification was then initiated by addition of 650 μ l of 100 mM sodium citrate buffer pH 5 containing 80 μ g ml⁻¹ tetracycline and 0.05 % (w/w) Cellic CTec3 cellulase (Novozymes). After 72 h of incubation at 50°C with shaking (1400 rpm), samples were centrifuged and the supernatant was filtered through 0.45- μ m nylon membrane centrifugal filters (VWR International, Radnor, PA) for glucose and xylose measurements, using high-performance liquid chromatography (HPLC). The system was equipped with an Aminex cation-exchange resin column HPX-87H, 300 \times 7.8 mm (Bio-Rad) and the eluent was 4 mM H₂SO₄ at a flow rate of 0.6 ml min⁻¹ at 60°C. Glucose and xylose were identified by refractive index and their amount quantified using 8-point calibration curves of authentic compounds. The same method was used for the pretreatment and saccharification of sorghum biomass. Wild-type sorghum plants (variety wheatland) were grown in the greenhouse until

full maturity and the biomass from entire plants (panicles removed) was processed into a powder as previously described (Tian et al., 2024). Saccharification assays were conducted on the raw biomass and extracted biomass obtained as described in 2.5.

2.9. Techno-economic analysis (TEA)

In this study, sorghum was selected as a representative crop for β KA accumulation due to its high biomass yield, natural drought tolerance, and water-use efficiency, alongside its relative ease to be engineered compared to other biomass crops such as Miscanthus. The feedstock cost is based on a higher biomass-yielding photoperiod sensitive sorghum line. *SuperPro Designer v14* was used to develop techno-economic models. The process flow diagram is shown in Fig. 2.

We assume that β KA accumulates uniformly throughout the entire plant, as indicated by its concentration in dry weight basis, which reflects average accumulation across all harvestable sorghum biomass. Additionally, we assume that β KA remains stable throughout the entire extraction process. The simulated process broadly includes the following steps: 1) size reduction; 2) extraction; and 3) separation and recovery. Following the approach described in Rorrer et al., (2022), ancillary facilities—such as those for steam generation, cooling agent supply, and utilities—are considered to be "over-the-fence" and their costs are directly included in the annual operating expenses (Supplementary Table S5). The costs of other raw materials used in this study are also listed in Supplementary Table S5, which are sourced from various studies as referenced and adjusted to the analysis year of 2023 using the Consumer Price Index (CPI) (United States Department of Labor, Bureau of Labor Statistics, 2024).

The simulated facility is sized to take in 2000 bone-dry metric tons (MT) per day of biomass sorghum feedstock (83.33 dry MT h⁻¹). Sorghum bales are first shredded and conveyed into a mixer containing a

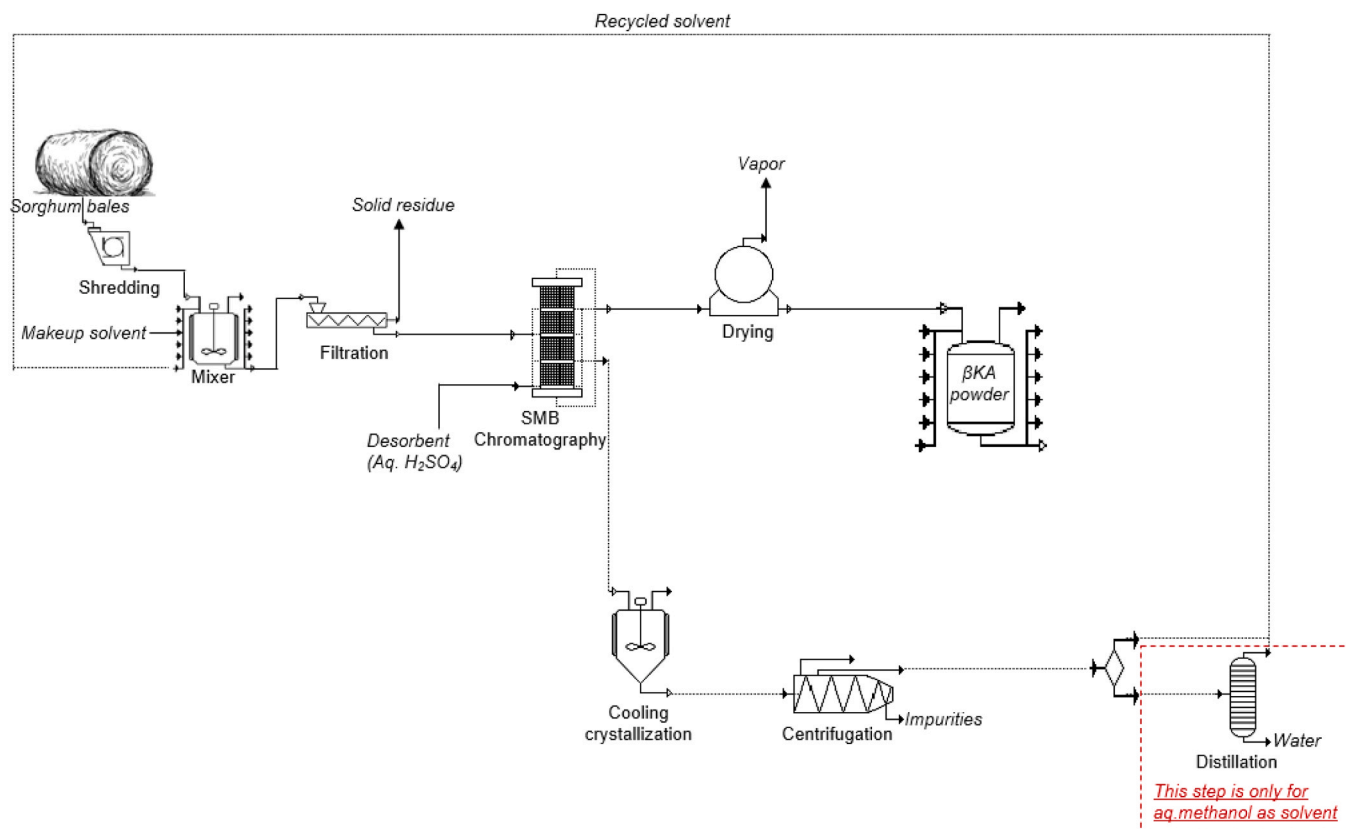


Fig. 2. Simplified process flow diagram of the techno-economic model of β KA extraction from engineered sorghum biomass. Aq. H₂SO₄: aqueous sulfuric acid; SMB: simulated moving bed.

solvent (either 80 % v/v aqueous methanol or water) at a solid loading of 24 % (dry wt/wt%). This loading ratio, which corresponds to ~284 mg dry biomass ml⁻¹, is higher than in our experimental setup, but it better represents the process intensification expected for large-scale industrial applications. Consistent with this study, there is a 45-min retention period in the mixer. This single 45-min stage rather than three separate 15-min stages minimizes solvent usage and equipment costs while ensuring thorough extraction. The extraction in the mixer occurs adiabatically at the recycled solvent's temperature (although the experiment was conducted at 70 °C to intentionally convert all the βKA to levulinic acid for easier quantification). A screw press subsequently separates the solid and liquid phases. The liquid phase, consisting in the solvent and soluble metabolites, is sent to simulated moving bed (SMB) chromatography for βKA recovery. The SMB chromatography produces a product stream of > 90 % βKA, with the balance being solvent, and the remaining solvent is removed in a dryer to produce a ~99 % βKA solid powder. The raffinate from SMB chromatography contains both solvent and impurities, requiring cooling crystallization (10 °C with freon as the cooling agent) to remove impurities such as extra metabolites and sulfuric acid (H₂SO₄) used in the eluent. Impurities crystallize out as solid particles and are then separated from the solvent via centrifugation, with the solids disposed of as waste. Solvent recovered from centrifugation is recycled for reuse in the extraction process.

To understand the cost impact of solvent loss and recovery this study compares recovery costs for two solvents: water and aqueous methanol. Using water in place of aqueous methanol as the solvent reduces the βKA recovery by 19 % (Supplementary Fig. S1), but no additional steps are needed before recycling, due to its homogenous nature. In contrast, when aqueous methanol is used, an extra distillation step is required to restore its original concentration, as it becomes diluted by the water used as a desorbent/eluent in SMB chromatography. To reduce energy consumption, only a portion of the solvent stream from centrifugation undergoes distillation. This stream is split into two parts: one is distilled to recover pure methanol, which is then blended with the remaining fraction to restore the methanol concentration to its original level. Makeup solvent is added during the next extraction process to compensate any loss incurred in the previous extraction.

The solid biomass residue removed after the screw press is a potential coproduct. The value of this solid biomass residue is a key question for any bioproduct that is extracted from plant tissue and its value influences the MSP of βKA. Rather than making an assumption about how the residue is used, this study explores how the economics of βKA production vary depending on solid residue value. The extraction facility is assumed to operate 24 h per day and 330 days per year (7920 h per year) for 30 years. The equipment purchase costs for each section were adjusted using an installation factor derived from Humbird et al. (2011) which was then followed by the calculation of direct and indirect costs, and the total capital investment. To determine the MSP of βKA for different scenarios, a cash flow analysis for the year of 2023 was conducted following the methodology outlined by Humbird et al. (2011), which sets the internal rate of return to 10 % and calculates MSP such that the net present value equals zero.

2.10. Statistical analyses

Statistical analyses were assessed as described in the figure legends. Student's *t* tests were performed using <https://www.graphpad.com/quickcalcs/ttest1/>.

3. Results

3.1. Transient expression of AroG, QsuB, PCA 3,4-dioxygenase (PcaHG), and 3-carboxy-cis,cis-muconate cycloisomerase (PcaB) enables βKA production in *Nicotiana benthamiana* leaves

Our previous study reported on the efficient overproduction of PCA in *N. benthamiana* leaves upon transient expression of plastid-targeted AroG and QsuB (Lin et al., 2021). This approach was used to test two potential routes for βKA biosynthesis (Fig. 1). As expected, using LC-MS analysis, the accumulation of PCA was observed in acid-hydrolyzed methanol extracts from leaves infiltrated with the two genes *aroG* and *qsuB* (Fig. 3). We subsequently co-expressed AroG and QsuB with either plastid-targeted PcaHG, PcaB, PcaC, and PcaD (Fig. 1, route 1) or MNX1, TsdC, and TsdD (Fig. 1, route 2) to assess the conversion of PCA into βKA. For route 2, expression of AroG, QsuB, MNX1, TsdC, and TsdD resulted in a small amount of βKA produced in leaves (1.1 mg g⁻¹ dry weight) despite the obvious depletion of PCA compared to the leaves only expressing AroG and QsuB (Fig. 3). We also detected the presence of the pathway intermediate hydroxyquinol in these leaves (~3.8 mg g⁻¹ dry weight), whereas β-hydroxy-cis,cis-muconate and maleylacetate could not be observed. These results indicate that MNX1 efficiently converts PCA into hydroxyquinol in *N. benthamiana*, but TsdC and/or TsdD poorly perform the subsequent step(s) for the conversion of hydroxyquinol into βKA. Alternatively, the intermediates β-hydroxy-cis,cis-muconate and maleylacetate may be unstable in plant tissues. On the other hand, for route 1, the data showed that over 95 % of PCA was efficiently converted into βKA upon expression of the *pcaH*, *pcaG*, *pcaB*, *pcaC*, and *pcaD* genes, resulting in βKA titers greater than 40 mg g⁻¹ dry weight, and thereby validating this metabolic pathway for βKA production in *planta*. Interestingly, a combinatorial approach for the co-expression of all aforementioned genes minus one revealed that neither *pcaC*, nor *pcaD* were necessary for βKA synthesis, indicating that unknown endogenous enzymes in *N. benthamiana* are capable of catalyzing the last two steps of the biosynthetic pathway (Fig. 3).

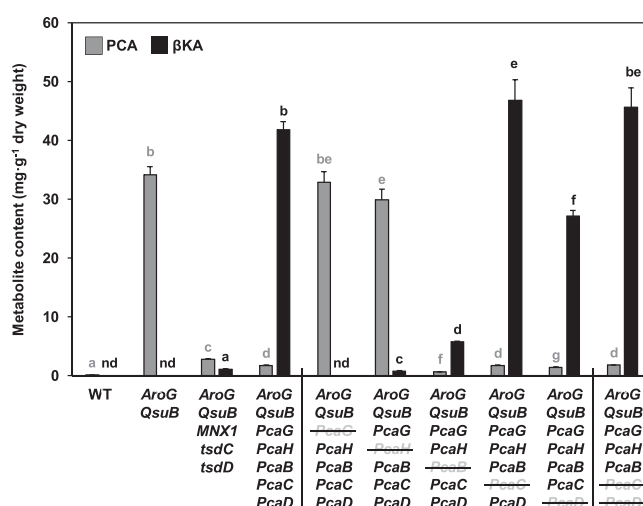


Fig. 3. *In planta* conversion of PCA into βKA in *N. benthamiana* leaves by transient expression of AroG, QsuB, and the proposed βKA biosynthetic enzymes PcaHG, PcaB, PcaC, and PcaD (route 1) or MNX1, TsdC, and TsdD (route 2). For route 1, a combinatorial approach showed that PcaC and PcaD are not required for βKA synthesis. Values are averages ± SE from four biological replicates (n = 4 plants). Letters represent significant differences (*P* < 0.05) using one-way ANOVA with post hoc Tukey HSD. Nd, not detected.

3.2. Stable expression of *PcaHG* and *PcaB* leads to β KA production in the *Arabidopsis QsuB-2* background

Based on the data obtained from transient expression assays in *N. benthamiana*, the *Arabidopsis* transgenic line *QsuB-2* expressing plastid-targeted *AroG* and *QsuB* (Umana et al., 2022) was transformed with a construct (*pAt β KA*) designed for the expression of plastid-targeted *PcaHG* and *PcaB* (Fig. 4). The 17.6-kb expression cassette contains the three genes *pcaH*, *pcaG*, and *pcaB* placed under the control of promoters active in stem tissues that produce lignified secondary cell walls Supplementary Table S3. First, matured senesced and dried stems from fourteen independent *QsuB-2 x pAt β KA* primary T0 transformants were subjected to a metabolite analysis to validate β KA production and identify the most promising lines. β KA titers in methanol extracts ranged from 0.1 to 6.6 mg g⁻¹ dry weight (Supplementary Fig. S2). No β KA could be detected in either the wild-type or the *QsuB-2* control line grown in the same conditions.

We then further characterized the top three β KA-producing lines in the T1 generation. First, using RT-PCR analysis, the expression of the *aroG*, *qsuB*, *pcaG*, *pcaH*, and *pcaB* transgenes was confirmed in stems from the three *QsuB-2 x pAt β KA* lines (Fig. 5A). Next, metabolites were extracted from matured stems to quantify PCA and β KA by LC-MS. PCA titers measured in acid-hydrolyzed extracts averaged ~90 mg g⁻¹ dry weight in the *QsuB-2* parental background and were significantly lower in the three *QsuB-2 x pAt β KA* lines (Fig. 5B). In addition, β KA titers ranged from 2.0 to 2.4 mg g⁻¹ dry weight in the *QsuB-2 x pAt β KA* lines (Fig. 5C).

3.3. Biomass from β KA producing plants displays improved saccharification without yield penalty

In accordance with previous reports showing significant lignin reductions in *Arabidopsis* lines expressing *QsuB* (Eudes et al., 2015; Lin et al., 2021), the *QsuB-2* parental background displayed a 53 % reduction in lignin content in comparison to the wild-type control, and a similar decrease, ranging from 52 % to 58 %, was observed in the *QsuB-2 x pAt β KA* transgenics (Fig. 6A). Biomass saccharification assays were conducted on stem biomass to evaluate the cell wall recalcitrance of the β KA producing lines. Following a hot water pretreatment and a 72-h enzymatic digestion, higher amounts of glucose and xylose were released from the biomass of the *QsuB-2* parental background and the three *QsuB-2 x pAt β KA* lines compared to the wild-type control (Fig. 6B). Saccharification improvements ranged from 191 % to 249 % for glucose and from 90 % to 121 % for xylose. This data shows a reduced biomass recalcitrance to enzymatic degradation, implying that less severe pretreatment and/or lower enzyme loadings could be employed to achieve optimal yields of fermentable sugars.

Moreover, although measurements of stem height at maturity

showed significant reductions in the *QsuB-2* parental background and the *QsuB-2 x pAt β KA* transgenics, total stem biomass dry weight was either not affected or even significantly higher compared to wild-type control plants (Fig. 7).

3.4. Techno-economic analysis

The β KA titer of 4 % on a dry weight basis achieved in *N. benthamiana* leaves was selected as the first scenario (Fig. 3). This titer was applied to sorghum for the purposes of the model as a hypothetical case. Fig. 8 illustrates the MSPs of β KA at this titer in sorghum, with variations in the selling price of the solid residues recovered after β KA extraction. For comparison, Baral et al. estimated sorghum prices from \$122 (silage) to \$167 (pellets)/bone dry metric ton delivered to the reactor throat at large-scale lignocellulosic biorefineries, including transportation, storage, and size reduction (Baral et al., 2020).

We found that, despite leading to a lower β KA extraction efficiency, water extraction led to more economically favorable outcomes relative to aqueous methanol extraction (Fig. 8). Avoiding methanol extraction not only eliminates the capital and energy-intensive recycling costs but also removes the need to purchase makeup methanol. The savings from these cost reductions substantially outweigh the yield loss of β KA.

Since water-only extraction resulted in better economic performance, an additional scenario analysis was conducted by adjusting the β KA titer to 0.25 %, a level achieved in the stable *QsuB-2 x pAt β KA* *Arabidopsis* line (Fig. 5C). The results of this analysis are shown in Fig. 9.

At 0.25 % β KA titer and with water extraction, if the selling price of the solid residue is set to match the feedstock purchase price (\$89/MT), the MSP of β KA would be \$34.49/kg. However, the residue has undergone processes that increase its value, namely delivery to a centralized facility and size reduction. If the residue selling price is increased by 63 % to \$145/MT, the MSP of β KA drops by 94 %, reaching \$2.04/kg (Fig. 9). For context, the average market price for adipic acid in 2017 was \$1.80/kg (Johnson et al., 2019), which is equivalent to \$2.24/kg in 2023 USD. Given the performance advantages of nylon-6, β K6 over nylon-6,6, β KA could be competitively priced at \$2.04/kg with a 0.25 % β KA titer in biomass and a residue selling price of \$145/MT. As noted earlier, the higher residue selling price compared to the feedstock purchase price can be justified by value of simplified residue logistics and potentially avoiding the need of further milling.

In addition to the logistics and size reduction advantages, the ease of biomass residue deconstruction to sugars may also be improved through the extraction process. As shown in Supplementary Fig. S3, the glucose yield from extracted biomass (solid residues) remaining after aqueous methanol extraction is 50 % higher using a hot water pretreatment and enzymatic saccharification compared to the original unextracted biomass material. These results suggest that the extraction process can reduce biomass recalcitrance, making it more suitable for conversion to

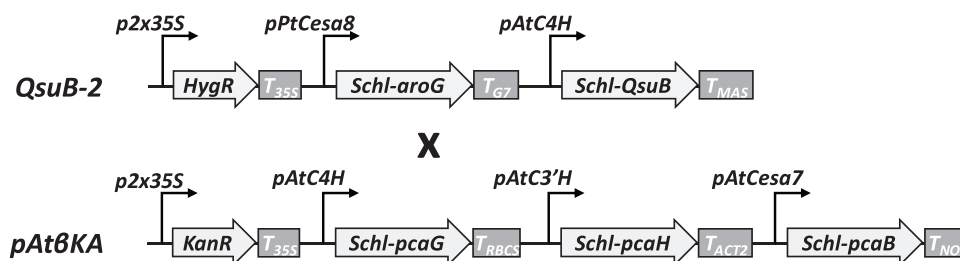


Fig. 4. Schematic representation of binary vectors used for *Arabidopsis* transformations. The *QsuB-2* construct was used for the production of PCA in wild-type *Arabidopsis* (Umana et al., 2022). The *pAt β KA* construct was used for the production of β KA in the *QsuB-2* *Arabidopsis* background. ‘Schl’ indicates plastid transit peptides. *p2x35S*, *pPtCesa8*, *pAtC4H*, *pAtC3'H*, and *pAtCesa7* designate the promoters of cauliflower mosaic virus 35S, poplar cellulose synthase 8 (Potri.004G059600), and *Arabidopsis* cinnamate 4-hydroxylase (At2G30490), coumarate 3'-hydroxylase (At2G40890), and cellulose synthase 7 (At5G17420) genes, respectively. *T_{35S}*, *T_{G7}*, *T_{MAS}*, *T_{NOS}*, *T_{RBCS}*, and *T_{ACT2}* designate the terminators of cauliflower mosaic virus 35S, *Agrobacterium* gene 7, mannopine synthase and nopaline synthase, and *Arabidopsis* Rubisco small subunit and Actin 2 genes, respectively. *HygR* and *KanR* denote the selectable marker genes used for plant selection using hygromycin and kanamycin, respectively.

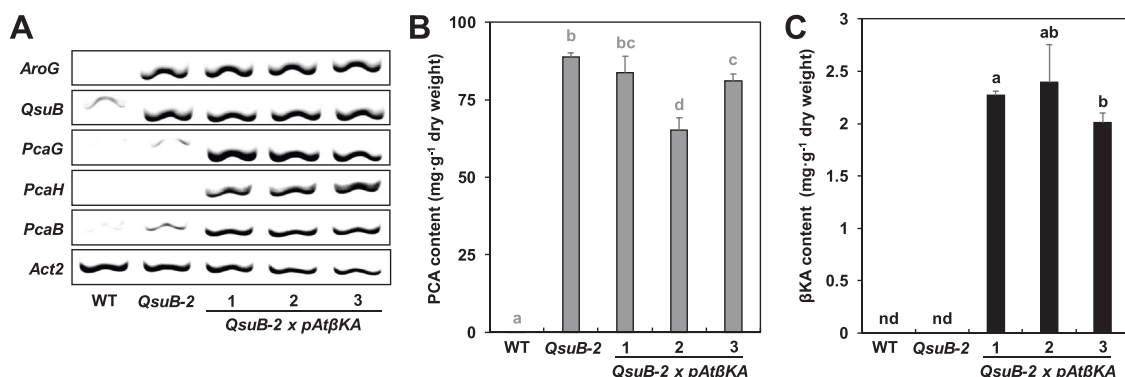


Fig. 5. *In planta* production of βKA in Arabidopsis stems resulting from the expression of PcaHG and PcaB in a transgenic *QsuB-2* background. (A) Detection by RT-PCR of *aroG*, *qsuB*, *pcaH*, *pcaG*, and *pcaB* transcripts in three independent lines containing the *pAtβKA* construct. The actin 2 gene (*Act2*) was used as a control. (B) PCA and (C) βKA titers in Arabidopsis wild-type (WT), *QsuB-2* parental background (*QsuB-2*), and *QsuB-2* x *pAtβKA* transformants. Values are averages ± SE from four biological replicates (n = 4 plants). Letters represent significant differences ($P < 0.05$) using one-way ANOVA with post hoc Tukey HSD. Nd, not detected.

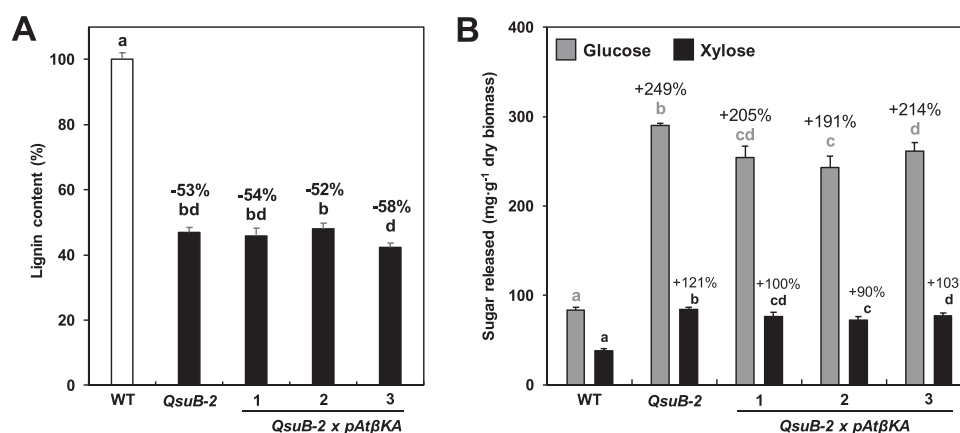


Fig. 6. (A) Lignin content in Arabidopsis wild-type (WT), *QsuB-2* parental background (*QsuB-2*), and *QsuB-2* x *pAtβKA* lines. Values are averages ± SE from four biological replicates (n = 4 plants). (B) Biomass saccharification of Arabidopsis wild-type (WT), *QsuB-2* parental background (*QsuB-2*), and *QsuB-2* x *pAtβKA* lines. Amounts of glucose and xylose released from biomass after 72-h enzymatic digestion are shown. Values are averages ± SE from five biological replicates (n = 5 plants). Percentage increases compared to wild-type are shown. Letters represent significant differences ($P < 0.05$) using one-way ANOVA with post hoc Tukey HSD.

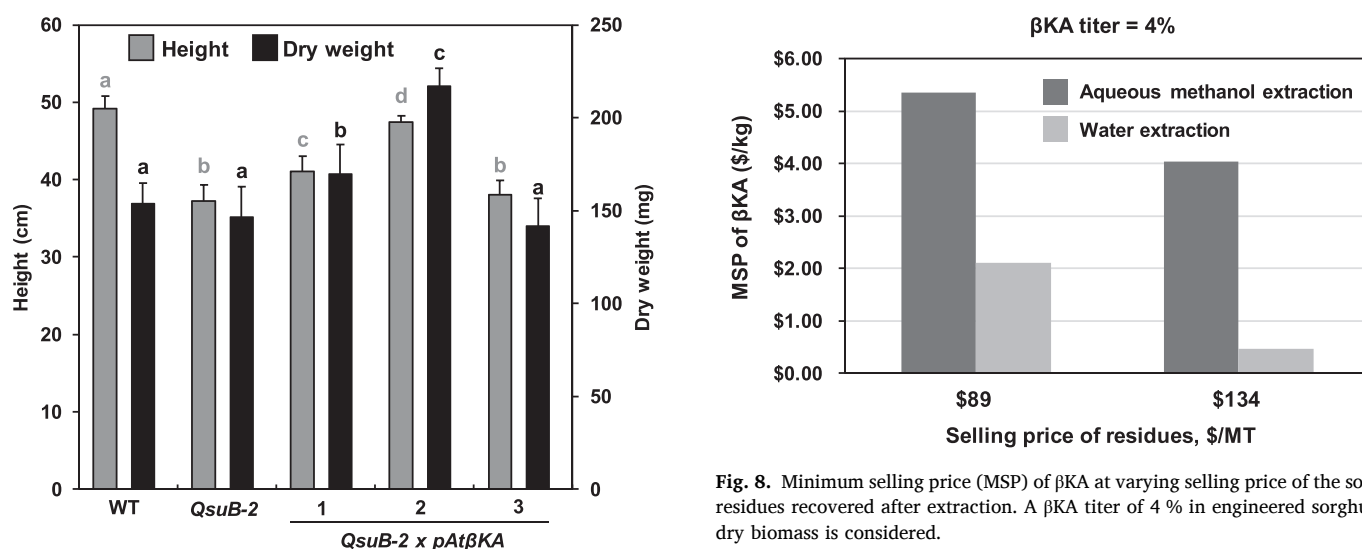


Fig. 7. Growth parameters (height and dry weight) of Arabidopsis wild-type (WT), *QsuB-2* parental background (*QsuB-2*), and *QsuB-2* x *pAtβKA* lines. Values are averages ± SE from eight biological replicates (n = 8 plants). Letters represent significant differences ($P < 0.05$) using one-way ANOVA with post hoc Tukey HSD.

Fig. 8. Minimum selling price (MSP) of βKA at varying selling price of the solid residues recovered after extraction. A βKA titer of 4% in engineered sorghum dry biomass is considered.

sugars, fuels, and other bioproducts. This indicates that βKA accumulated *in planta*, could compete with fossil-derived adipic acid on a cost basis, depending on the size of the residue market and premium placed on post-extraction residues. Additionally, given the reported titer in this

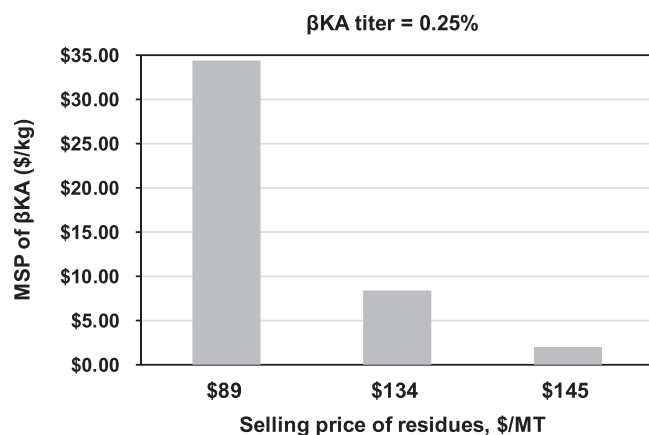


Fig. 9. Minimum selling price (MSP) of beta-KA at varying selling price of the solid residues recovered after water extraction. A beta-KA titer of 0.25 % in engineered sorghum dry biomass is considered.

study, the MSP of *in planta*-synthesized beta-KA can be lower than the MSP of beta-KA produced through microbial methods, which was estimated to be \$1.94/kg (Rorrer et al., 2022) in 2014 USD (\$2.50/kg in 2023 USD) based on an optimistic production titer assumption (90 g·L⁻¹, or approximately 3.5X the maximum reported titer of 26 g·L⁻¹). With water extraction, a 0.25 % beta-KA titer *in planta* can reach \$2.04/kg if the residue sells for at least \$145/MT (63 % above the price paid for incoming feedstock). At a 4 % titer, beta-KA extracted with water reaches \$2.12/kg at a residue price of just \$89/MT.

4. Discussion and conclusions

Beta-ketoadipate represents a promising building block chemical for the manufacturing of nylon-6,6 analogs and we demonstrate in this study that plants can be engineered to accumulate it. *In planta* synthesis of beta-KA is achieved via conversion of PCA, as previously reported in several engineered microbial strains (Johnson et al., 2019; Rorrer et al., 2022; Sullivan et al., 2022). In plants, PCA can be overproduced from 3-dehydroshikimate by heterologous expression of 3-dehydroshikimate dehydratase (QsuB), which also results in lignin reduction (Eudes et al., 2015). This approach is relevant to the bioenergy field since reducing lignin or manipulating its composition facilitates the deconstruction of biomass feedstocks into simple sugars for the production of advanced bioproducts and biofuels (Eudes et al., 2014). Co-expression of QsuB with feedback-resistant 3-deoxy-D-arabinoheptulosonate 7-phosphate synthase (AroG) further enhances PCA production, making this approach appealing for the *in planta* accumulation of valuable PCA-derived chemicals (Lin et al., 2021; Umana et al., 2022). Interestingly, the reduction of lignin achieved by QsuB expression is maintained despite AroG expression, indicating that increased carbon flux through the shikimate pathway supports PCA accumulation but not lignin synthesis in the AroG-QsuB Arabidopsis line (i.e. QsuB-2). These observations are consistent with previous results showing that constitutive expression of feedback-resistant AroG did not increase lignin content in Arabidopsis stems, although the lignin precursors phenylalanine and shikimate were higher (Tzin et al., 2012). This phenomenon could be the result of tight regulations in the plant phenylpropanoid pathway that affect, for example, the entry point phenylalanine ammonia-lyase or the available pool of phenylalanine (Lynch et al., 2017; Zhang and Liu, 2015).

We tested two potential routes for conversion of PCA into beta-KA *in planta* (Fig. 1). The pathway that begins with the formation of hydroxyquinol catalyzed by MNX1 showed limited potential towards beta-KA production, despite the obvious depletion of PCA (Fig. 3). The low titers of hydroxyquinol and beta-KA measured in this pathway suggest that the downstream enzymes TsdC and TsdD are poorly active in plastids and/

or the pathway intermediates are unstable or are converted into different metabolites in plant tissues. To the best of our knowledge, this pathway has never been tested in microbial hosts for beta-KA production and it may be well-suited for *R. jostii* RHA1, which is the source of the *tsdC* and *tsdD* genes and a promising strain for biomanufacturing (Cappelletti et al., 2020). Moreover, some enzymes similar to TsdC and TsdD recently characterized in white-rot fungi could be tested for beta-KA production in heterologous hosts (Kuatsjah et al., 2024). In the case of the pathway initiated by the intradiol cleavage of PCA catalyzed by PcaHG, we observed in *N. benthamiana* a nearly complete conversion of PCA into beta-KA using the strong constitutive 35S promoter for gene expression (Fig. 3). To implement this pathway in Arabidopsis, we selected stem-specific promoters for gene expression to limit the risk of undesirable growth defects (Fig. 4). However, even though this approach resulted in Arabidopsis lines accumulating beta-KA without any biomass yield reductions (Fig. 5C, Fig. 7), a significant amount of PCA remained in these lines compared to the PCA content measured in the QsuB-2 parental background (Fig. 5B). Considering that PcaG and PcaH form a heterodimer for ring cleavage activity, their synchronized spatial and temporal expression is probably required for efficient PCA conversion. We predicted that the two promoters selected for *pcaG* and *pcaH* expression in Arabidopsis stems (*pAtC4H* and *pAtC3'H*, respectively) would confer optimal and overlapping expression patterns since they drive the expression of genes encoding two enzymes that are part of a P450 enzyme complex during lignin biosynthesis (Gou et al., 2018). However, we cannot exclude that the ~2-kb *pAtC4H* and *pAtC3'H* promoter regions used in this work are missing some regulatory elements needed for full promoter activity. Alternatively, polyprotein expression systems could be tested to coordinate PcaG and PcaH co-expression and facilitate their interaction (Zhang et al., 2017; 2019). The efficient cleavage of PCA represents an important step for beta-KA synthesis since PCA is known to be exported from the plastid to the cytosol and converted into a wide range of conjugates (Akyuz Turumtay et al., 2024). Moreover, considering that our *de novo* beta-KA pathway is confined to plastids, integrating the corresponding biosynthetic genes as operons into the chloroplast genome could achieve optimal co-expression and enhance beta-KA synthesis (Fuentes et al., 2018). Lastly, we found that the conversion of the pathway intermediate gamma-carboxymuconolactone into beta-KA can occur in plant tissues without expressing PcaC and PcaD (Fig. 1 route 1, Fig. 3), suggesting that endogenous and promiscuous plant decarboxylase(s) and hydrolase(s) catalyze the last two steps in this pathway, or a single enzyme with dual activity as previously described in *Rhodococcus opacus* 1CP (PcaL) (Eulberg et al., 1998). Whether such conversion takes place inside the plastid or in another compartment after the export of gamma-carboxymuconolactone remains unknown, and no enzyme showing sequence homology with either PcaC, PcaD, or PcaL could be retrieved from Arabidopsis databases (data not shown). Conversely, as previously noticed in earlier studies, we cannot exclude that gamma-carboxymuconolactone decarboxylates spontaneously into beta-ketoadipate enol-lactone (Ornston and Stanier, 1966). Importantly, accumulation of beta-KA in *N. benthamiana* and Arabidopsis indicates that plant tissues possess low, if any, beta-KA degradation activity.

Currently, the most promising bioenergy crop background for producing beta-KA at a larger scale is the engineered QsuB poplar, which accumulates up to 1.2 % PCA on a dry weight basis and has ~20 % less lignin in woody tissues (Lin et al., 2022a; Unda et al., 2022). Another approach for increasing PCA in plants is the co-expression of plastid-targeted chorismate pyruvate-lyase (UbiC) and *p*-hydroxybenzoate hydroxylase (PobA), as previously shown in Arabidopsis (Eudes et al., 2016). To this end, the functional expression of UbiC has already been validated in both hybrid poplar and sorghum for the accumulation of *p*-hydroxybenzoate (Lin et al., 2022b; Mottiar et al., 2023).

Finally, the TEA indicated that the accumulation titer, type of solvent used, and the value of solid residues remaining after extraction substantially influence the economic performance of beta-KA production *in*

planta. If further increasing the accumulation titer proves to be a limitation for commercially-relevant crops, identifying applications for solid biomass residues where ease of deconstruction is valued can enable a competitive process. Moreover, a biological funneling approach leveraging engineered microbial strains could be utilized to produce additional β KA from unconverted pathway intermediates such as PCA. For β KA extraction and the extraction of products accumulated *in planta* more broadly, the use of cheaper solvents should be explored as a mechanism to reduce the cost and energy requirements. With careful consideration of solvent choice, opportunities for process intensification, and producing a value-added biomass residue, this study shows that currently-demonstrated β KA titers offer a path to performance-advantaged renewable polymers.

CRedit authorship contribution statement

Amyerick Eudes: Writing – review & editing, Writing – original draft, Validation, Supervision, Methodology, Investigation, Funding acquisition, Data curation, Conceptualization. **Corinne D. Scown:** Writing – review & editing, Writing – original draft, Validation, Supervision, Methodology, Investigation, Funding acquisition, Data curation, Conceptualization. **Jaya Tripathi:** Writing – review & editing, Writing – original draft, Validation, Investigation, Formal analysis, Data curation. **Sami Kazaz:** Writing – review & editing, Writing – original draft, Validation, Investigation, Formal analysis, Data curation. **Monikaben Nimavat:** Formal analysis. **İrem Pamukçu:** Formal analysis. **Edward E. K. Baidoo:** Writing – review & editing, Validation, Supervision, Methodology. **Emine Akyuz Turumtay:** Validation, Formal analysis. **Yang Tian:** Writing – review & editing, Validation, Methodology, Formal analysis. **Dylan Chin:** Formal analysis. **Halbay Turumtay:** Formal analysis.

Funding

This material is based upon work supported by the Joint BioEnergy Institute, U.S. Department of Energy, Office of Science, Biological and Environmental Research Program under Award Number DE-AC02-05CH11231 with Lawrence Berkeley National Laboratory. This study was also supported by the U. S. Department of Energy, Energy Efficiency and Renewable Energy, Bioenergy Technologies Office.

Declaration of Competing Interest

The authors declare the following financial interests/personal relationships which may be considered as potential competing interests: Corinne D. Scown reports a relationship with Cyklos Materials that includes: equity or stocks. Other authors declare that they have no known competing financial interests or personal relationships that could have appeared to influence the work reported in this paper.

Acknowledgements

Authors are grateful to Novozymes for providing the Cellic CTec3 cellulase.

Appendix A. Supporting information

Supplementary data associated with this article can be found in the online version at [doi:10.1016/j.jbiotec.2025.04.008](https://doi.org/10.1016/j.jbiotec.2025.04.008).

Data availability

Data will be made available on request.

References

- Akyuz Turumtay, E., Turumtay, H., Tian, Y., Lin, C.-Y., Chai, Y.N., Louie, K.B., Chen, Y., Lipzen, A., Harwood, T., Satish Kumar, K., Bowen, B.P., Wang, Q., Mansfield, S.D., Blow, M.J., Petzold, C.J., Northen, T.R., Mortimer, J.C., Scheller, H.V., Eudes, A., 2024. Expression of dehydroshikimate dehydratase in poplar induces transcriptional and metabolic changes in the phenylpropanoid pathway. *J. Exp. Bot.* 75, 4960–4977. <https://doi.org/10.1093/jxb/erae251>.
- Baral, N.R., Dahlberg, J., Putnam, D., Mortimer, J.C., Scown, C.D., 2020. Supply cost and life-cycle greenhouse gas footprint of dry and ensiled biomass sorghum for biofuel production. *ACS Sustain. Chem. Eng.* 8, 15855–15864. <https://doi.org/10.1021/acsschemeng.0c03784>.
- Bechtold, N., Pelletier, G., 1998. In planta Agrobacterium-mediated transformation of adult Arabidopsis thaliana plants by vacuum infiltration. *Methods Mol. Biol.* 82, 259–266. <https://doi.org/10.1385/0-89603-391-0-259>.
- Belcher, M.S., Vuu, K.M., Zhou, A., Mansoori, N., Agosto Ramos, A., Thompson, M.G., Scheller, H.V., Loqué, D., Shih, P.M., 2020. Design of orthogonal regulatory systems for modulating gene expression in plants. *Nat. Chem. Biol.* 16, 857–865. <https://doi.org/10.1038/s41589-020-0547-4>.
- Cappelletti, M., Presentato, A., Piacenza, E., Firrincieli, A., Turner, R.J., Zannoni, D., 2020. Biotechnology of *Rhodococcus* for the production of valuable compounds. *Appl. Microbiol. Biotechnol.* 104, 8567–8594. <https://doi.org/10.1007/s00253-020-10861-z>.
- Del Cerro, C., Erickson, E., Dong, T., Wong, A.R., Eder, E.K., Purvine, S.O., Mitchell, H.D., Weitz, K.K., Markillie, L.M., Burnet, M.C., Hoyt, D.W., Chu, R.K., Cheng, J.-F., Ramirez, K.J., Katahira, R., Xiong, W., Himmel, M.E., Subramanian, V., Linger, J.G., Salvachúa, D., 2021. Intracellular pathways for lignin catabolism in white-rot fungi. *Proc. Natl. Acad. Sci. USA* 118. <https://doi.org/10.1073/pnas.2017381118>.
- Eudes, A., Berthomieu, R., Hao, Z., Zhao, N., Benites, V.T., Baidoo, E.E.K., Loqué, D., 2018. Production of muconic acid in plants. *Metab. Eng.* 46, 13–19. <https://doi.org/10.1016/j.ymben.2018.02.002>.
- Eudes, A., Liang, Y., Mitra, P., Loqué, D., 2014. Lignin bioengineering. *Curr. Opin. Biotechnol.* 26, 189–198. <https://doi.org/10.1016/j.copbio.2014.01.002>.
- Eudes, A., Pereira, J.H., Yogiswara, S., Wang, G., Teixeira Benites, V., Baidoo, E.E.K., Lee, T.S., Adams, P.D., Keasling, J.D., Loqué, D., 2016. Exploiting the substrate promiscuity of hydroxycinnamoyl-CoA:shikimate hydroxycinnamoyl transferase to reduce lignin. *Plant Cell Physiol.* 57, 568–579. <https://doi.org/10.1093/pcp/pcw016>.
- Eudes, A., Sathitsuksanoh, N., Baidoo, E.E.K., George, A., Liang, Y., Yang, F., Singh, S., Keasling, J.D., Simmons, B.A., Loqué, D., 2015. Expression of a bacterial 3-dehydroshikimate dehydratase reduces lignin content and improves biomass saccharification efficiency. *Plant Biotechnol. J.* 13, 1241–1250. <https://doi.org/10.1111/pbi.12310>.
- Eulberg, D., Lakner, S., Golovleva, L.A., Schlömann, M., 1998. Characterization of a protocatechuate catabolic gene cluster from *Rhodococcus opacus* 1CP: evidence for a merged enzyme with 4-carboxymuconolactone-decarboxylating and 3-oxoadipate enol-lactone-hydrolyzing activity. *J. Bacteriol.* 180, 1072–1081. <https://doi.org/10.1128/JB.180.5.1072-1081.1998>.
- Fenster, J.A., Werner, A.Z., Tay, J.W., Gillen, M., Schirokauer, L., Hill, N.C., Watson, A., Ramirez, K.J., Johnson, C.W., Beckham, G.T., Cameron, J.C., Eckert, C.A., 2022. Dynamic and single cell characterization of a CRISPR-interference toolset in *Pseudomonas putida* KT2440 for β -ketoacid production from p-coumarate. *Metab. Eng. Commun.* 15, e00204. <https://doi.org/10.1016/j.mec.2022.e00204>.
- Fuentes, P., Armarego-Marriott, T., Bock, R., 2018. Plastid transformation and its application in metabolic engineering. *Curr. Opin. Biotechnol.* 49, 10–15. <https://doi.org/10.1016/j.copbio.2017.07.004>.
- Gou, M., Ran, X., Martin, D.W., Liu, C.-J., 2018. The scaffold proteins of lignin biosynthetic cytochrome P450 enzymes. *Nat. Plants* 4, 299–310. <https://doi.org/10.1038/s41477-018-0142-9>.
- Hao, Z., Yogiswara, S., Wei, T., Benites, V.T., Sinha, A., Wang, G., Baidoo, E.E.K., Ronald, P.C., Scheller, H.V., Loqué, D., Eudes, A., 2021. Expression of a bacterial 3-dehydroshikimate dehydratase (QsuB) reduces lignin and improves biomass saccharification efficiency in switchgrass (*Panicum virgatum* L.). *BMC Plant Biol.* 21, 56. <https://doi.org/10.1186/s12870-021-02842-9>.
- Harwood, C.S., Parales, R.E., 1996. The beta-ketoacid pathway and the biology of self-identity. *Annu. Rev. Microbiol.* 50, 553–590. <https://doi.org/10.1146/annurev.micro.50.1.553>.
- Hasanbeigi, A., Sibal, A., 2023. Stopping a Super-Pollutant: N₂O Emissions Abatement From Global Adipic Acid Production. *Global Efficiency Intelligence, Florida, United States*.
- Holesova, Z., Jakubkova, M., Zavadikova, I., Zeman, I., Tomaska, L., Nosek, J., 2011. Gentisate and 3-oxoadipate pathways in the yeast *Candida parapsilosis*: identification and functional analysis of the genes coding for 3-hydroxybenzoate 6-hydroxylase and 4-hydroxybenzoate 1-hydroxylase. *Microbiology* 157, 2152–2163. <https://doi.org/10.1099/mic.0.048215-0>.
- Humbird, D., Davis, R., Tao, L., Kinchin, C., Hsu, D., Aden, A., Schoen, P., Lukas, J., Olthoff, B., Worley, M., Sexton, D., Dudgeon, D., 2011. Process design and economics for biochemical conversion of lignocellulosic biomass to ethanol: Dilute-acid pretreatment and enzymatic hydrolysis of corn stover. National Renewable Energy Laboratory (NREL), Golden, CO (United States). <https://doi.org/10.2172/1013269>.
- Johnson, C.W., Salvachúa, D., Rorrer, N.A., Black, B.A., Vardon, D.R., St. John, P.C., Cleveland, N.S., Dominick, G., Elmore, J.R., Grundl, N., Khanna, P., Martinez, C.R., Michener, W.E., Peterson, D.J., Ramirez, K.J., Singh, P., VanderWall, T.A., Wilson, A. N., Yi, X., Bidy, M.J., Bomble, Y.J., Guss, A.M., Beckham, G.T., 2019. Innovative chemicals and materials from bacterial aromatic catabolic pathways. *Joule*. <https://doi.org/10.1016/j.joule.2019.05.011>.

- Kasai, D., Araki, N., Motoi, K., Yoshikawa, S., Iino, T., Imai, S., Masai, E., Fukuda, M., 2015. γ -Resorcyate catabolic-pathway genes in the soil actinomycete *Rhodococcus jostii* RHA1. *Appl. Environ. Microbiol.* 81, 7656–7665. <https://doi.org/10.1128/AEM.02422-15>.
- Kitagawa, W., Kimura, N., Kamagata, Y., 2004. A novel *p*-nitrophenol degradation gene cluster from a gram-positive bacterium, *Rhodococcus opacus* SAO101. *J. Bacteriol.* 186, 4894–4902. <https://doi.org/10.1128/JB.186.15.4894-4902.2004>.
- Kondo, M.Y., Montagna, L.S., Morgado, G.F., de, M., Castilho, A.L.G., de, Batista, L.A.P., dos, S., Botelho, E.C., Costa, M.L., Passador, F.R., Rezende, M.C., Ribeiro, M.V., 2022. Recent advances in the use of polyamide-based materials for the automotive industry. *Pol. Ímeros* 32. <https://doi.org/10.1590/0104-1428.20220042>.
- Kuatsjah, E., Schwartz, A., Zahn, M., et al., 2024. Biochemical and structural characterization of enzymes in the 4-hydroxybenzoate catabolic pathway of lignin-degrading white-rot fungi. *Cell Rep.* 43, 115002.
- Lin, C.-Y., Geiselman, G.M., Liu, D., Magurudeniya, H.D., Rodriguez, A., Chen, Y.-C., Pidatala, V., Unda, F., Amer, B., Baidoo, E.E.K., Mansfield, S.D., Simmons, B.A., Singh, S., Scheller, H.V., Gladden, J.M., Eudes, A., 2022a. Evaluation of engineered low-lignin poplar for conversion into advanced bioproducts. *Biotechnol. Biofuels* 15, 145. <https://doi.org/10.1186/s13068-022-02245-4>.
- Lin, C.-Y., Tian, Y., Nelson-Vasilchik, K., Hague, J., Kakumanu, R., Lee, M.Y., Pidatala, V. R., Trinh, J., De Ben, C.M., Dalton, J., Northen, T.R., Baidoo, E.E.K., Simmons, B.A., Gladden, J.M., Scown, C.D., Putnam, D.H., Kausch, A.P., Scheller, H.V., Eudes, A., 2022b. Engineering sorghum for higher 4-hydroxybenzoic acid content. *Metab. Eng. Commun.* 15, e00207. <https://doi.org/10.1016/j.mec.2022.e00207>.
- Lin, C.-Y., Vuu, K.M., Amer, B., Shih, P.M., Baidoo, E.E.K., Scheller, H.V., Eudes, A., 2021. In-planta production of the biodegradable polyester precursor 2-pyrone-4,6-dicarboxylic acid (PDC): Stacking reduced biomass recalcitrance with value-added co-product. *Metab. Eng.* 66, 148–156. <https://doi.org/10.1016/j.ymben.2021.04.011>.
- Liu, C.-J., Eudes, A., 2022. Lignin synthesis and bioengineering approaches toward lignin modification. In: *Advances in Botanical Research*. Elsevier. <https://doi.org/10.1016/bs.abr.2022.02.002>.
- Lynch, J.H., Orlova, I., Zhao, C., Guo, L., Jaini, R., Maeda, H., Akhtar, T., Cruz-Lebron, J., Rhodes, D., Morgan, J., Pilot, G., Pichersky, E., Dudareva, N., 2017. Multifaceted plant responses to circumvent Phe hyperaccumulation by downregulation of flux through the shikimate pathway and by vacuolar Phe sequestration. *Plant J.* 92, 939–950. <https://doi.org/10.1111/tpj.13730>.
- Maeda, H., Dudareva, N., 2012. The shikimate pathway and aromatic amino acid biosynthesis in plants. *Annu. Rev. Plant Biol.* 63, 73–105. <https://doi.org/10.1146/annurev-arplant-042811-105439>.
- Mottiar, Y., Karlen, S.D., Goacher, R.E., Ralph, J., Mansfield, S.D., 2023. Metabolic engineering of *p*-hydroxybenzoate in poplar lignin. *Plant Biotechnol. J.* 21, 176–188. <https://doi.org/10.1111/pbi.13935>.
- Nicholson, S.R., Rorrer, N.A., Uekert, T., Avery, G., Carpenter, A.C., Beckham, G.T., 2023. Manufacturing energy and greenhouse gas emissions associated with United States consumption of organic petrochemicals. *ACS Sustain. Chem. Eng.* 11, 2198–2208. <https://doi.org/10.1021/acscchemeng.2c05417>.
- O'Neill, E.C., Kelly, S., 2017. Engineering biosynthesis of high-value compounds in photosynthetic organisms. *Crit. Rev. Biotechnol.* 37, 779–802. <https://doi.org/10.1080/07388551.2016.1237467>.
- Okamura-Abe, Y., Abe, T., Nishimura, K., Kawata, Y., Sato-Izawa, K., Otsuka, Y., Nakamura, M., Kajita, S., Masai, E., Sonoki, T., Katayama, Y., 2016. Beta-ketoacid and muconolactone production from a lignin-related aromatic compound through the protocatechuate 3,4-metabolic pathway. *J. Biosci. Bioeng.* 121, 652–658. <https://doi.org/10.1016/j.jbiosc.2015.11.007>.
- Ornston, L.N., Stanier, R.Y., 1966. The conversion of catechol and protocatechuate to beta-ketoacidipate by *Pseudomonas putida*. *J. Biol. Chem.* 241, 3776–3786. [https://doi.org/10.1016/S0021-9258\(18\)99839-X](https://doi.org/10.1016/S0021-9258(18)99839-X).
- Polen, T., Spelberg, M., Bott, M., 2013. Toward biotechnological production of adipic acid and precursors from biorenewables. *J. Biotechnol.* 167, 75–84. <https://doi.org/10.1016/j.jbiotec.2012.07.008>.
- Qi, G., Wang, D., Yu, L., Tang, X., Chai, G., He, G., Ma, W., Li, S., Kong, Y., Fu, C., Zhou, G., 2015. Metabolic engineering of 2-phenylethanol pathway producing fragrance chemical and reducing lignin in *Arabidopsis*. *Plant Cell Rep.* 34, 1331–1342. <https://doi.org/10.1007/s00299-015-1790-0>.
- Rorrer, N.A., Notonier, S.F., Knott, B.C., Black, B.A., Singh, A., Nicholson, S.R., Kinchin, C.P., Schmidt, G.P., Carpenter, A.C., Ramirez, K.J., Johnson, C.W., Salvachúa, D., Crowley, M.F., Beckham, G.T., 2022. Production of β -ketoacidipate from glucose in *Pseudomonas putida* KT2440 for use in performance-advanced nylons. *Cell Rep. Phys. Sci.* 3, 100840. <https://doi.org/10.1016/j.xcrp.2022.100840>.
- Shende, V.V., Bauman, K.D., Moore, B.S., 2024. The shikimate pathway: gateway to metabolic diversity. *Nat. Prod. Rep.* 41, 604–648. <https://doi.org/10.1039/d3np00037k>.
- Shih, P.M., Vuu, K., Mansoori, N., Ayad, L., Louie, K.B., Bowen, B.P., Northen, T.R., Loqué, D., 2016. A robust gene-stacking method utilizing yeast assembly for plant synthetic biology. *Nat. Commun.* 7, 13215. <https://doi.org/10.1038/ncomms13215>.
- Shimizu, A., Tanaka, K., Fujimori, M., 2000. Abatement technologies for N₂O emissions in the adipic acid industry. *Chemos. - Glob. Change Sci.* 2, 425–434. [https://doi.org/10.1016/S1465-9972\(00\)00024-6](https://doi.org/10.1016/S1465-9972(00)00024-6).
- Sparkes, I.A., Rונים, J., Kearns, A., Hawes, C., 2006. Rapid, transient expression of fluorescent fusion proteins in tobacco plants and generation of stably transformed plants. *Nat. Protoc.* 1, 2019–2025. <https://doi.org/10.1038/nprot.2006.286>.
- Spence, E.M., Scott, H.T., Dumond, L., Calvo-Bado, L., di Monaco, S., Williamson, J.J., Persinoti, G.F., Squina, F.M., Bugg, T.D.H., 2020. The hydroxyquinol degradation pathway in *Rhodococcus jostii* RHA1 and *Agrobacterium* species is an alternative pathway for degradation of protocatechuic acid and lignin fragments. *Appl. Environ. Microbiol.* 86. <https://doi.org/10.1128/AEM.01561-20>.
- Sullivan, K.P., Werner, A.Z., Ramirez, K.J., Ellis, L.D., Bussard, J.R., Black, B.A., Brandner, D.G., Bratti, F., Buss, B.L., Dong, X., Haugen, S.J., Ingraham, M.A., Konev, M.O., Michener, W.E., Miscall, J., Pardo, I., Woodworth, S.P., Guss, A.M., Román-Leshkov, Y., Stahl, S.S., Beckham, G.T., 2022. Mixed plastics waste valorization through tandem chemical oxidation and biological funneling. *Science* 378, 207–211. <https://doi.org/10.1126/science.abo4626>.
- Suzuki, Y., Otsuka, Y., Araki, T., Kamimura, N., Masai, E., Nakamura, M., Katayama, Y., 2021. Lignin valorization through efficient microbial production of β -ketoacidipate from industrial black liquor. *Bioresour. Technol.* 337, 125489. <https://doi.org/10.1016/j.biortech.2021.125489>.
- Suzuki, S., Suzuki, Y., Yamamoto, N., Hattori, T., Sakamoto, M., Umezawa, T., 2009. High-throughput determination of thioglycolic acid lignin from rice. *Plant Biotechnol.* 26, 337–340. <https://doi.org/10.5511/plantbiotechnology.26.337>.
- Tian, Y., Gao, Y., Turumtay, H., Turumtay, E.A., Chai, Y.N., Choudhary, H., Park, J.-H., Wu, C.-Y., De Ben, C.M., Dalton, J., Louie, K.B., Harwood, T., Chin, D., Vuu, K.M., Bowen, B.P., Shih, P.M., Baidoo, E.E.K., Northen, T.R., Simmons, B.A., Huttmacher, R., Atim, J., Putnam, D.H., Scown, C.D., Mortimer, J.C., Scheller, H.V., Eudes, A., 2024. Engineered reduction of S-adenosylmethionine alters lignin in sorghum. *Biotechnol. Biofuels* 17, 128. <https://doi.org/10.1186/s13068-024-02572-8>.
- Tian, Y., Yang, M., Lin, C.-Y., Park, J.-H., Wu, C.-Y., Kakumanu, R., De Ben, C.M., Dalton, J., Vuu, K.M., Shih, P.M., Baidoo, E.E.K., Temple, S., Putnam, D.H., Scheller, H.V., Scown, C.D., Eudes, A., 2022. Expression of dehydroshikimate dehydratase in sorghum improves biomass yield, accumulation of protocatechuate, and biorefinery economics. *ACS Sustain. Chem. Eng.* 10, 12520–12528. <https://doi.org/10.1021/acscchemeng.2c01160>.
- Tzin, V., Malitsky, S., Zvi, M.M.B., Bedair, M., Sumner, L., Aharoni, A., Galili, G., 2012. Expression of a bacterial feedback-insensitive 3-deoxy-D-arabino-heptulosonate 7-phosphate synthase of the shikimate pathway in *Arabidopsis* elucidates potential metabolic bottlenecks between primary and secondary metabolism. *New Phytol.* 194, 430–439. <https://doi.org/10.1111/j.1469-8137.2012.04052.x>.
- U.S. Bureau of Labor Statistics, 2024. Inflation & Prices. Retrieved August 13, 2024, from (<https://www.bls.gov/data/#prices>).
- Umama, G.E., Perez, J.M., Unda, F., Lin, C.-Y., Sener, C., Karlen, S.D., Mansfield, S.D., Eudes, A., Ralph, J., Donohue, T.J., Nogueira, D.R., 2022. Biological funneling of phenolics from transgenic plants engineered to express the bacterial 3-dehydroshikimate dehydratase (qsuB) gene. *Front. Chem. Eng.* 4. <https://doi.org/10.3389/fceng.2022.1036084>.
- Unda, F., Mottiar, Y., Mahon, E.L., Karlen, S.D., Kim, K.H., Loqué, D., Eudes, A., Ralph, J., Mansfield, S.D., 2022. A new approach to zip-lignin: 3,4-dihydroxybenzoate is compatible with lignification. *New Phytol.* 235, 234–246. <https://doi.org/10.1111/nph.18136>.
- Vagholkar, P., 2016. Nylon (Chemistry, Properties and Uses). *Int. J. Sci. Res.* 5, 349–351.
- Varghese, M., Grimstaff, M.W., 2022. Beyond nylon 6: polyamides via ring opening polymerization of designer lactam monomers for biomedical applications. *Chem. Soc. Rev.* 51, 8258–8275. <https://doi.org/10.1039/d1cs00930c>.
- Wells, T., Ragauskas, A.J., 2012. Biotechnological opportunities with the β -ketoacidipate pathway. *Trends Biotechnol.* 30, 627–637. <https://doi.org/10.1016/j.tibtech.2012.09.008>.
- Werner, A.Z., Clare, R., Mand, T.D., Pardo, I., Ramirez, K.J., Haugen, S.J., Bratti, F., Dexter, G.N., Elmore, J.R., Huenemann, J.D., Peabody, G.L., Johnson, C.W., Rorrer, N.A., Salvachúa, D., Guss, A.M., Beckham, G.T., 2021. Tandem chemical deconstruction and biological upcycling of poly(ethylene terephthalate) to β -ketoacidipate by *Pseudomonas putida* KT2440. *Metab. Eng.* 67, 250–261. <https://doi.org/10.1016/j.ymben.2021.07.005>.
- Werner, A.Z., Cordell, W.T., Lohme, C.W., Klein, B.C., Singer, C.A., Tan, E.C.D., Ingraham, M.A., Ramirez, K.J., Kim, D.H., Pedersen, J.N., Johnson, C.W., Pfleger, B.F., Beckham, G.T., Salvachúa, D., 2023. Lignin conversion to β -ketoacidipate by *Pseudomonas putida* via metabolic engineering and bioprocess development. *Sci. Adv.* 9, ead0053. <https://doi.org/10.1126/sciadv.adj0053>.
- Wu, W., Dutta, T., Varman, A.M., Eudes, A., Manalansan, B., Loqué, D., Singh, S., 2017. Lignin valorization: two hybrid biochemical routes for the conversion of polymeric lignin into value-added chemicals. *Sci. Rep.* 7, 8420. <https://doi.org/10.1038/s41598-017-07895-1>.
- Yan, K., Wang, J., Wang, Z., Yuan, L., 2023. Bio-based monomers for amide-containing sustainable polymers. *Chem. Commun.* 59, 382–400. <https://doi.org/10.1039/d2cc05161c>.
- Yang, M., Liu, D., Baral, N.R., Lin, C.-Y., Simmons, B.A., Gladden, J.M., Eudes, A., Scown, C.D., 2022. Comparing in planta accumulation with microbial routes to set targets for a cost-competitive bioeconomy. *Proc. Natl. Acad. Sci. USA* 119, e2122309119. <https://doi.org/10.1073/pnas.2122309119>.
- Yuan, L., Grotewold, E., 2015. Metabolic engineering to enhance the value of plants as green factories. *Metab. Eng.* 27, 83–91. <https://doi.org/10.1016/j.ymben.2014.11.005>.
- Zhang, B., Han, Z., Kumar, S., Gupta, M., Su, W.W., 2019. Intein-ubiquitin chimeric domain for coordinated protein coexpression. *J. Biotechnol.* 304, 38–43. <https://doi.org/10.1016/j.jbiotec.2019.08.006>.
- Zhang, X., Liu, C.-J., 2015. Multifaceted regulations of gateway enzyme phenylalanine ammonia-lyase in the biosynthesis of phenylpropanoids. *Mol. Plant* 8, 17–27. <https://doi.org/10.1016/j.molp.2014.11.001>.
- Zhang, B., Rapolu, M., Kumar, S., Gupta, M., Liang, Z., Han, Z., Williams, P., Su, W.W., 2017. Coordinated protein co-expression in plants by harnessing the synergy between an intein and a viral 2A peptide. *Plant Biotechnol. J.* 15, 718–728. <https://doi.org/10.1111/pbi.12670>.